THE JOURNAL OF BIOLOGICAL CHEMISTRY VOL. 282, NO. 29, pp. 20887–20896, July 20, 2007

Regulation of Transcript Elongation through Cooperative and Ordered Recruitment of Cofactors*[S]

Received for publication, February 16, 2007, and in revised form, May 23, 2007 Published, JBC Papers in Press, May 29, 2007, DOI 10.1074/jbc.M701420200

Manish Sharma[1], **Anuja A. George**[1], **Badri N. Singh, Naresh C. Sahoo, and Kanury V. S. Rao**[2]

From the Immunology Group, International Centre for Genetic Engineering and Biotechnology, Aruna Asaf Ali Marg, New Delhi 110067, India

We studied the regulation of murine *CD80*, a gene whose basal transcriptional status was characterized by the presence of a stalled RNA polymerase II complex on the promoter-proximal region. Stimulus-induced activation of productive elongation involved a complex interplay of regulated events that included a synergy between ordered cofactor recruitment. This cascade of recruitments was initiated through the engagement of transcription factor NF-κB, leading to the temporal association of histone acetyltransferases and the consequent selective acetylation of a transcription start site downstream nucleosome. This in turn culminated into the nucleosomal association of Brd4-associated P-TEFb, a protein complex containing kinase specific for serine 2 of Rbp 1, the largest subunit of the carboxyl-terminal domain of RNA polymerase II. The consequent phosphorylation of serine 2 residues in CTD by CDK9 in the P-TEFb complex then facilitated escape of polymerase II into the productive elongation phase. Thus, the cooperative mechanisms that integrate between independent pathways characterize regulation of the elongation step of transcription, thereby providing another level at which specificity of gene regulation can be achieved.

The transcription cycle involves distinct stages of preinitiation, initiation, promoter clearance, elongation, and termination. The vast majority of studies, however, have focused primarily on elucidating mechanisms regulating preinitiation and initiation. Although the subsequent steps of elongation and mRNA processing have received considerably less attention (1), more recent findings are revealing the dynamic and regulated nature of these processes (2, 3). Thus, processivity of RNA polymerase II (Pol II)[3] is now known to be regulated by a class of proteins collectively termed as transcription elongation factors. Regulation by such factors can either be active or passive, depending upon whether they affect the rate of catalysis by Pol II (2).

The carboxyl-terminal domain (CTD) of Rpb1, the largest subunit of Pol II, also represents a key player in regulating entry of the latter into the productive elongation phase. CTD consists of multiple repeats of the heptapeptide sequence YSPTSPS, and hyperphosphorylation of serine residues in this repeat region is a hallmark of the productive elongation phase of the transcription cycle (2, 4). Ser^2 and Ser^5 residues of CTD have been identified as the major phosphorylation sites (5), whereas CDK7, CDK8, and CDK9 are the major CTD kinases (6). Recent studies have revealed that these two modifications can be detected differentially in the various regions of the gene and are associated with distinct stages of the transcription cycle (7–9).

Here we examined the mechanism of regulation of expression of the murine CD80 gene from a newly identified transcription start site. CD80 is a key costimulatory molecule that is expressed primarily on the professional antigen presenting cells in an inducible manner (10). Previous studies on the murine CD80 promoter have identified the presence of two transcription start sites located at 315 (TS1) and 1742 (TS2) nucleotides upstream of the translation start site (11, 12). Our present studies reveal the operation of a post-initiation mechanism of regulation involving a preassembled preinitiation complex and a stalled RNA polymerase II in the promoter-proximal regions. Importantly, the activation of transcription, marked by the release of stalled polymerase II, was preceded by a series of interlinked recruitment events that included transcription factor NF-κB, P/CAF, and CBP/P300 histone acetyltransferases and CDK9, a kinase specific for serine 2 of CTD. Thus, the cooperative and ordered recruitment of the protein cofactors served for the stimulus-dependent regulation of transcription elongation from this newly identified transcription start site.

EXPERIMENTAL PROCEDURES

Cell Culture and Reagents—FO cells (ATCC, Manassas, VA) were maintained in Dulbecco's modified Eagle's medium (Invitrogen) supplemented with 10% fetal bovine serum and 1× penicillin/streptomycin. The cells were stimulated by directly adding 10 μg/ml of the anti-CD40 antibody to the cells in complete medium. For the inhibition experiments, the cells were pretreated for 2 h prior to stimulation with either 300 μM capsaicin, cycloheximide (10 μg/ml), or 5,6-dichloro-1-β-D-ribofuranosyl-benzimidazole (DRB) (50 nM) (purchased from Sigma). The source of the various antibodies used in this manuscript, as well as the sequences of primers used for the various experiments, are listed in supplemental Table S1.

RNA Isolation and RT-PCR—Total RNA was isolated with TRIzol (Invitrogen) and digested with RNase free DNase I prior to reverse transcription reaction. No RT control was performed

* The costs of publication of this article were defrayed in part by the payment of page charges. This article must therefore be hereby marked "*advertisement*" in accordance with 18 U.S.C. Section 1734 solely to indicate this fact.
[S] The on-line version of this article (available at http://www.jbc.org) contains supplemental Figs. S1 and S2 and Table S1.
[1] Recipients of a research fellowship from the Council of Scientific and Industrial Research.
[2] To whom correspondence should be addressed. Tel.: 91-11-26176680; Fax: 91-11-26715114; E-mail: kanury@icgeb.res.in.
[3] The abbreviations used are: Pol II, polymerase II; CTD, carboxyl-terminal domain; TS, transcription start site; RT, reverse transcription; ChIP, chromatin immunoprecipitation; siRNA, small interfering RNA; nt, nucleotide(s); LM, ligation-mediated; MNase, micrococcal nuclease.

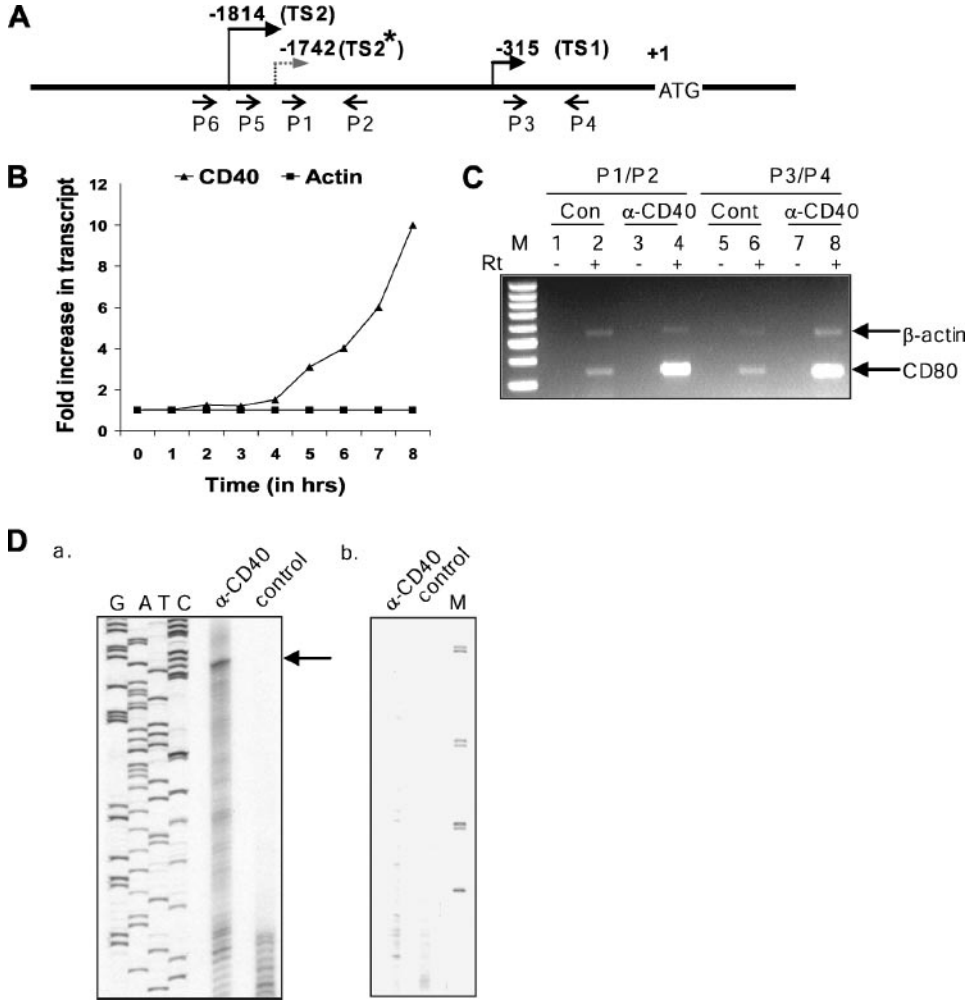

FIGURE 1. **Selective up-regulation of the CD80 transcript from TS2 in CD40-stimulated FO cells.** *A*, schematic representation of the two transcription start sites TS1 and TS2 (see text for details) and the different primers employed for analysis. The position of previously reported transcription start site has been indicated as *TS2**. The A residue of the first ATG codon (translation start site) was chosen as the reference and numbered +1. All further numbering was done with this convention. *B*, real time RT-PCR analysis, for the CD80 transcript, performed with the RNA isolated from the cells stimulated for indicated duration of time. *C*, RT-PCR with the indicated primer pairs (illustrated in *A*) employed to monitor the two expected transcripts originating at TS1 and TS2. The cells were stimulated with CD40 for 6 h. *D*, *panel a*, primer extension analysis, with end-labeled P2 primer, to monitor the enrichment in transcript from TS2 start site in CD40-stimulated and unstimulated cells (indicated in the Fig.). A sequencing ladder was employed to estimate size of the product. *Panel b*, the primer extension results obtained with labeled primer P4 and RNA from stimulated and unstimulated cells (control; *Con* or *Cont*). Labeled MspI-digested pBR322 fragments were used as molecular mass markers (*lane M*).

for each preparation. The manufacturer's instructions were followed for real time PCR using QuantiTect SYBR Green RT-PCR kit, (Qiagen) and RT-PCR using a Qiagen One-Step RT-PCR kit.

Chromatin Immunoprecipitation (ChIP) Assay—The ChIP procedure was carried out following the manufacturer's instructions (Upstate Biotechnology, Inc., Lake Placid, NY) with some modifications. Briefly, following specific stimulus, 3×10^6 cells were fixed with 1% formaldehyde for 10 min at 37 °C and quenched with 0.125 M glycine for 10 min at room temperature. Chromatin was sheared to an average size of <500 bp and precleared with protein A-agarose beads. The soluble chromatin was incubated overnight with 2–3 μg of antibody followed by incubation with the blocked beads. The immune complexes were collected by centrifugation and washed following the manufacturer's protocol. Input and immunoprecipitated chromatin samples were reverse cross-linked by incubating at 65 °C overnight in presence of 200 mM NaCl. Following proteinase K digestion, DNA was extracted with phenol/chloroform and precipitated with ethanol. Precipitated DNA was diluted serially, analyzed by PCR consisting of 28–32 amplification cycles, and resolved on agarose gel. The antibodies and the primer sequences employed have been listed in supplemental Table S1.

Nuclease Digestions, Ligation-mediated (LM)-PCR, Nucleosome Mapping, and $KmnO_4$ Footprinting—Micrococcal nuclease (MNase) and restriction enzyme digestion followed by LM-PCR was performed as described previously (13) with slight modifications. The amplification cycles employed were 20 (restriction enzyme), 18 (DNase I), and 22 (MNase).

Mononucleosomes were isolated from formaldehyde fixed cells as described previously (14) with the modification that nuclei were digested with 150 units of MNase at 37 °C for 30 min. For each Southern hybridization, 20 μg of purified MNase-digested DNA was used.

$KMnO_4$ treatment of the cells was performed at final concentrations of 2.5 and 5 mM with 2 min of incubation at room temperature. Following quenching with β-mercaptoethanol and piperidine cleavage, first strand synthesis was performed prior to ligation with unidirectional linker and LM-PCR.

siRNA—Target specific siRNA were purchased from Santa Cruz Biotechnology, Inc. or Dharmacon Inc. and transfected using SuperFect kit (Qiagen) at 10 μg/5×10^6 cells as recommended by the manufacturer. The negative control siRNA was targeted against green fluorescent protein. After 24–48 h in culture, the cells were employed for respective experiments. Western blotting was performed to monitor the efficiency of transfection.

RESULTS

CD40-dependent Up-regulation Of CD80 Is Initiated from a Novel Start Site—Fig. 1*A* provides a schematic representation of the murine CD80 promoter, indicating the positions of both TS1 and TS2. To examine induction of the murine CD80 transcript, we stimulated the plasmacytoma cell line, FO, with anti-CD40 antibodies. As shown in Fig. 1*B*, accumulation of CD80

mRNA could be first detected by 5 h, with its levels continuing to increase thereafter. Parallel experiments where cells were treated with cycloheximide prior to stimulation revealed that induction of the CD80 transcript did not require *de novo* protein synthesis (supplemental Fig. S1*A*).

To further characterize the transcript, we next performed RT-PCR using the two distinct primer pairs P1/P2 and P3/P4, illustrated in Fig. 1*A*, and designed to amplify the two anticipated transcripts originating from either TS1 or TS2. Amplification with both primer pairs was obtained (Fig. 1*C*), suggesting either that the product was selectively derived from TS2 or that it represented the sum of transcripts originating from both the initiation sites. To resolve between these two possibilities, we next performed a primer extension analysis using either the P2 or the P4 primer. A primer extension product was obtained with P2 (Fig. 1*D*, *panel a*) but not with the labeled P4 primer (Fig. 1*D*, *panel b*), suggesting that the CD40 mRNA preparation did not include a transcript originating from TS1. Interestingly, however, the primer extension product obtained with the P2 primer revealed a discrepancy in size of ~70 nt from that expected for a transcript being generated from the previously described position of TS2 (12) (illustrated as *TS2** in Fig. 1*A*). This was further verified by 5′ rapid amplification of cDNA ends experiments wherein sequencing of the resultant product identified the correct position of TS2 to be located at 72 nt upstream of its previously described location (supplemental Fig. S1*B*). Additional validation of this finding was obtained through RT-PCR employing primers upstream of P1 (supplemental Fig. S1*C*). Importantly, the presence of a single extension product with primer P2 also rules out the presence of multiple start sites in this region. Thus, from the results described here, the correct position of TS2 appears to be −1814 nt with respect to the translation start site (Fig. 1*A*). Further, stimulation of FO cells with anti-CD40 specifically induces transcription of CD80 from this site.

The TS2-proximal Promoter Is Organized into Three Translationally Positioned Nucleosomes—The chromatin environment represents at least one of the critical factors that exercise transcriptional control over a given gene (15). We therefore examined the TS2-proximal region for its nucleosomal organization. Initial experiments involved a low resolution analysis where Southern blotting was performed on *in vivo* MNase-digested nuclear DNA. Seven independent probes spanning the promoter region from −3320 to −1086 nt (Fig. 2*A*, *panel a*) were employed after first ascertaining that they hybridize with comparable efficiency to a cloned fragment of the CD80 promoter. Three of these yielded a positive signal in Southern blot experiments, indicating that the corresponding regions *in vivo* were resistant to MNase digestion (Fig. 2*A*, *panel b*). In subsequent experiments, soluble chromatin was immunoprecipitated with antibodies specific to either histone H3, histone H4, or YY1 (the latter as a negative control). Immunoprecipitated DNA was then released by reverse cross-linking prior to subjecting it to dot blot hybridization with these seven probes. The hybridization profile obtained here (Fig. 2*A*, *panel c*) was similar to that observed in Fig. 2*A* (*panel b*), further supporting that the protection observed for these three regions likely derives from their organization into nucleosomes.

By employing ligation-mediated PCR on mononucleosomal preparations, we were able to map the boundaries of these nucleosomes. Thus, these three nucleosomes, designated as 1, 2, and 3, could be positioned between −1395 to −1540, −2209 to −2354, and −2599 to −2744, respectively, relative to the translation start site (Fig. 2, *B* and *C*). To further confirm these positions, we also isolated DNA fragments from mononucleosome preparations that had first been immunoprecipitated with antibodies against either H3 or H4. Although these fragments yielded a PCR amplification product with primer pairs designed to amplify the 135-bp core nucleosome, this was not the case when any of the primers was substituted with one that was immediately outside the identified nucleosomal region (supplemental Fig. S1, *E* and *F*). Thus, these cumulative results establish the existence of three translationally positioned nucleosomes in the regions that flank TS2.

Interestingly, stimulation of cells with anti-CD40 led to selective changes in acetylation status only at nucleosome 1, with no such change at nucleosomes 2 and 3. This was revealed from mononucleosome ChIP experiments employing antibodies directed against various acetylated derivatives of H3 and H4 histones. For nucleosome 1, acetylation at lysines 18, 23, and 27 of H3 were the first stimulation-induced events observed (Fig. 2*D*). Acetylation at lysines 9 and 14 was also detected by 4 h of stimulation, which then persisted over the remainder of the experiment. Finally, the lysine tail of H4 was found to be constitutively acetylated, although no further attempts were made to delineate the residues involved. Thus, stimulation of cells with anti-CD40 resulted in dynamic changes in acetylation status specifically at nucleosome 1.

Polymerase Is Stalled at the TS2-proximal Region—To probe the mechanism by which anti-CD40 induces CD80 expression from TS2, we next examined for the recruitment of the basal transcription machinery. The cells were stimulated with anti-CD40 for varying times, and ChIP assays were performed using antibodies either against TATA-box-binding protein, TFIIB, or Pol II. Irrespective of the dilution employed, an equal and persistent signal was obtained with proximal promoter-specific primers for all the three antibodies (Fig. 3*A*). This suggested a constitutive occupancy by the basal Pol II machinery at the TS2-proximal promoter region. Constitutive occupancy of this promoter region could also be confirmed by *in vivo* DNase I footprinting experiments (supplemental Fig. S2*A*). Further, as shown in Fig. 3*A*, stimulation did not lead to any further increase in the extent of association of these proteins with the promoter. These ChIP experiments were subsequently repeated with primers designed to amplify ~320 bp in different regions of both the promoter and the coding sequences, with several dilutions of the immunoprecipitated DNA. A typical profile is illustrated in Fig. 3*B*, which reveals that TFIIB signal remained primarily localized to the proximal promoter region over the time course of the experiment. In contrast, the signal for Pol II increased in a time-dependent manner over the exon and the 3′-untranslated region. Thus, although Pol II was primarily localized to the promoter-proximal region in unstimulated cells, stimulation with anti-CD40 resulted in its redistribution over the entire gene.

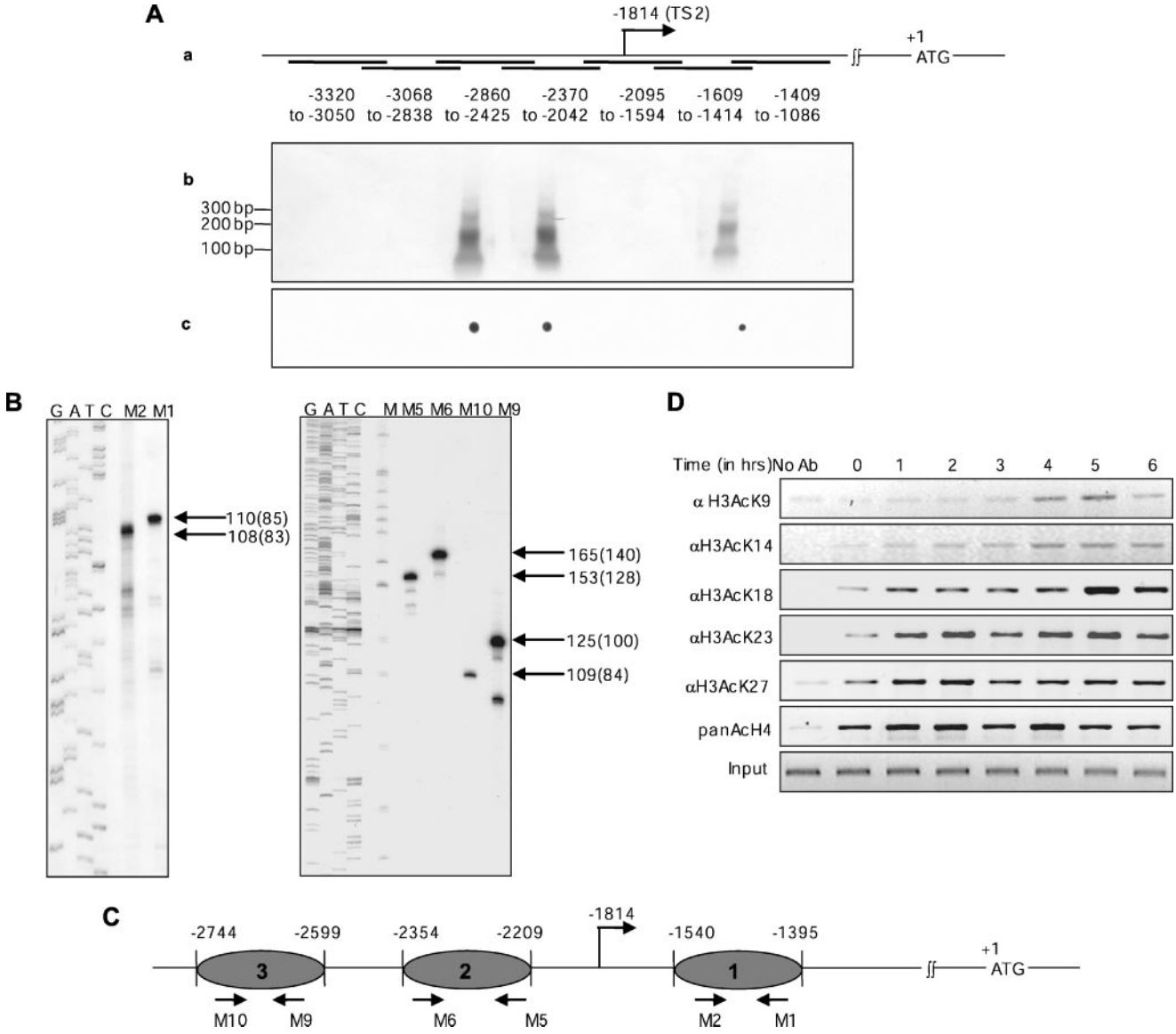

FIGURE 2. **Nucleosome organization of the CD80 promoter and stimulus-dependent change in acetylation profile of specific nucleosome.** *A*, *panel a*, represents the probes used for low resolution nucleosome positioning (not to scale). *Panel b*, Southern hybridization with the probes, as indicated in *panel a*, and the mononucleosome sized DNA generated by extensive MNase digestion of the isolated nuclei from unstimulated cells. *Panel c*, dot blot analysis with the same probes and H3 bound DNA generated by immunoprecipitating with an antibody specific to H3 core histone; following extensive MNase digestion of the cross-linked nuclei from unstimulated cells. *B*, fine positioning of nucleosomes using LM-PCR. The length of the products using the primers indicated in *C* are numbered on the *right*, and the *numbers* in *parentheses* correspond to the lengths of the products minus the 25-bp linker. *C*, schematic representation of the positioned nucleosomes and the primers employed (not to scale) in LM-PCR experiments. *D*, mononucleosome ChIP assay with antibodies directed to acetylated forms of the indicated lysine residues, in a time-dependent manner. The primers specific to each nucleosome were employed for amplification, but those depicted in the figure correspond to amplification obtained when primers specific to nucleosome 1 were employed. The specificity of immunoprecipitation was ensured in parallel experiments where the primary antibody was omitted (*No Ab*).

A stalled polymerase has also been shown to associate with the existence of an open complex in the regions corresponding to the site of stalling (16). Thus, to additionally verify the presence of a stalled Pol II in promoter-proximal regions, we also performed *in vivo* $KMNO_4$ footprinting assays to establish stimulus-specific open complexes in the promoter-proximal regions. The presence of unique *in vivo* $KMNO_4$-sensitive T residues could indeed be detected in the TS2 downstream region (Fig. 3*C*), indicative of the presence of an open complex. Further, the sensitivity of the T residues in the region ~200 bp downstream of TS2 showed a marked decrease in $KMNO_4$ sensitivity upon stimulation of cells, supporting the likelihood of this region being the site of stalling of Pol II in unstimulated cells. Thus, these cumulative findings reveal the operation of a post-initiation mechanism of regulation of transcription from TS2.

CD80 Expression Is Dependent on Cofactor Recruitment at the Promoter—In view of the previously described significance of both NF-κB and HMG(I)Y during CD80 up-regulation (17, 18), we next monitored for their time-dependent recruitment at the CD80 promoter following stimulation of cells with anti-CD40. In repeated ChIP experiments we observed increased recruitment of both the p65 and p50 subunits of NF-κB by 2 h of stimulation time, and this association then persisted over the

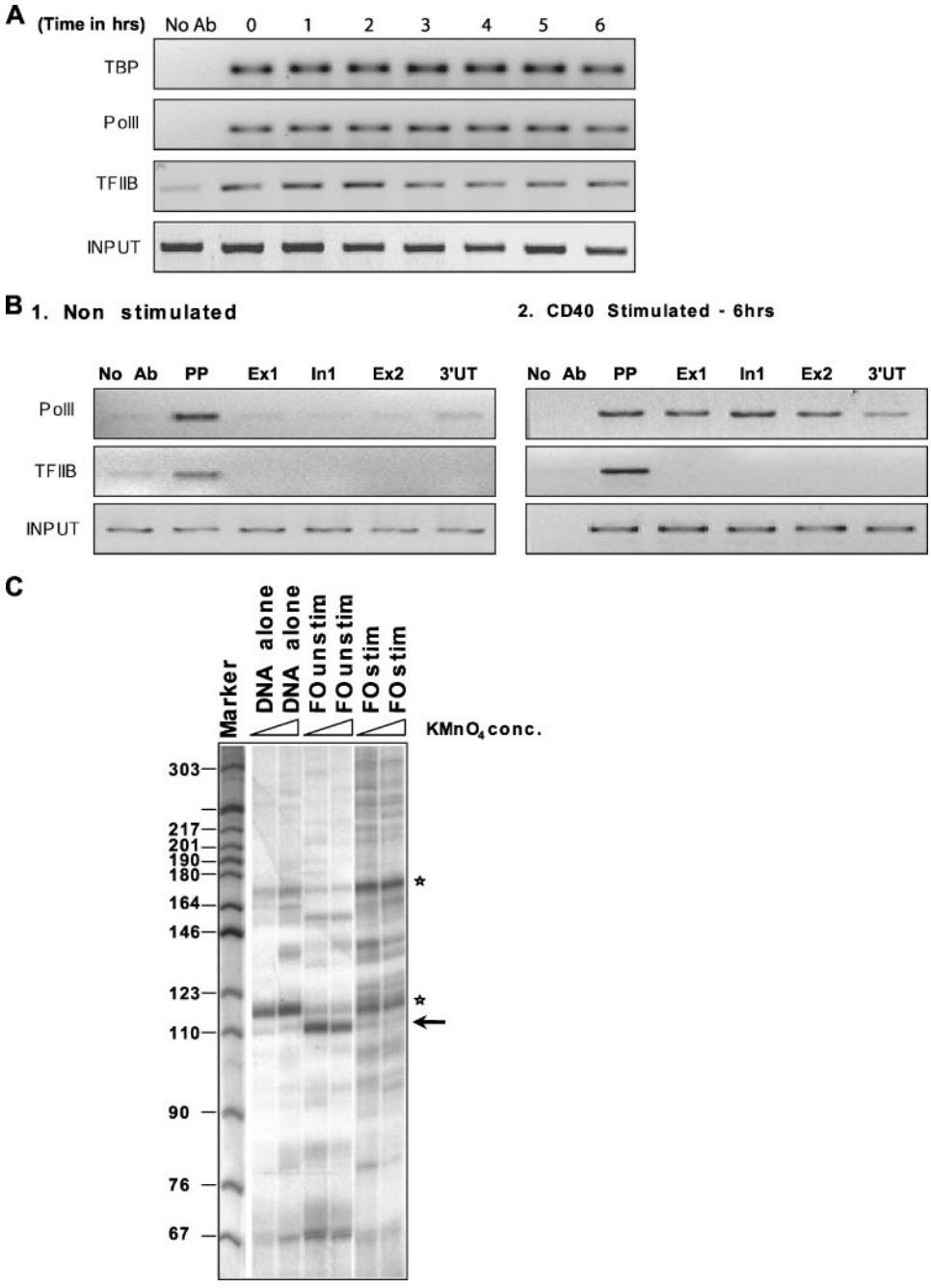

FIGURE 3. **Stalled Pol II on the TS2 promoter-proximal regions.** *A*, ChIP assays, with the indicated antibodies, performed in the cells stimulated for the indicated durations of time. Primer pairs in the TS2-proximal region were employed for amplification. The *No Ab* lane represents the immunoprecipitation specificity control where primary antibody was omitted. *B*, amplification results of primers across the gene, as indicated in the figure and the DNA generated following ChIP with the antibodies to Pol II and TFIIB. *C*, $KMnO_4$ foot printing to probe for the presence of an open complex in the TS2-proximal regions. A region, ~200 nucleotides downstream of TS2, showed a marked decrease in $KMnO_4$ sensitivity of T residues (indicated by an *arrow*) following stimulation with CD40. The *bands* indicated by *asterisks* represent the $KMnO_4$-sensitive T residues that could be detected even when the isolated DNA was used (*lanes 1* and *2*) and were employed as the internal controls for the normalization. Labeled MspI-digested pBR322 fragments were employed as molecular mass markers. All of the *lanes* are from the same gel. The marker lane is aligned.

remainder of the experiment (Fig. 4*A*). In contrast HMG(I)Y was constitutively associated with the promoter region, but it dissociated by 1 h of stimulation. Importantly, siRNA-mediated silencing of p65 expression abrogated the CD40-dependent induction of CD80 (Fig. 4*B*), implicating an obligatory role for NF-κB recruitment in this process.

An inspection of the TS2-proximal regions revealed the presence of a conserved NF-κB-binding consensus site located between +50 to +60 nt relative to TS2. The ability of this site to interact with NF-κB was initially established by performing electrophoretic mobility shift assay, supershifts, and cross-competition with a known target oligonucleotide for NF-κB binding (not shown). This result was subsequently confirmed by Scanning ChIP assays with anti-p65 or anti-p50 antibodies and cross-linked soluble chromatin subjected to Sau3A1 digestion to ensure multiple directed cleavages on the promoter prior to immunoprecipitation. For PCR, primer pairs designed to amplify in the expected Sau3A1 fragments (Fig. 4*C*, *panel a*) of the CD80 promoter were employed whereas primers pairs across the Sau3A1 site served as the controls. As shown in Fig. 4*C* (*panel b*), amplification was obtained only in the region around +55, suggesting that CD40-dependent recruitment of NF-κB occurred at this site. H3 served as the positive control and YY1 as the negative control in these experiments. In separate *in vitro* footprinting experiments with the purified recombinant protein, we also localized the HMG(I)Y-binding site to a region spanning between −1714 and −1709 nt (supplemental Fig. S2*B*).

Our observations in Fig. 2*D* that stimulation of cells with anti-CD40 resulted in the specific modulation of the acetylation profile at nucleosome 1 also prompted us to examine for the recruitment of histone acetyltransferases. This was achieved through mononucleosome ChIP assays. As shown in Fig. 4*D*, an increased association of P/CAF with the promoter could be detected by 1 h of stimulation. These levels peaked by 3 h and then declined thereafter. Dissociation of P/CAF was accompanied by the corresponding recruitment of both CBP and P300 (Fig. 4*D*). These latter events were detected by 5 h of stimulation, coinciding with the time point at which CD40-dependent transcription was initiated. To ascertain whether histone acetyltransferase recruitment was relevant to

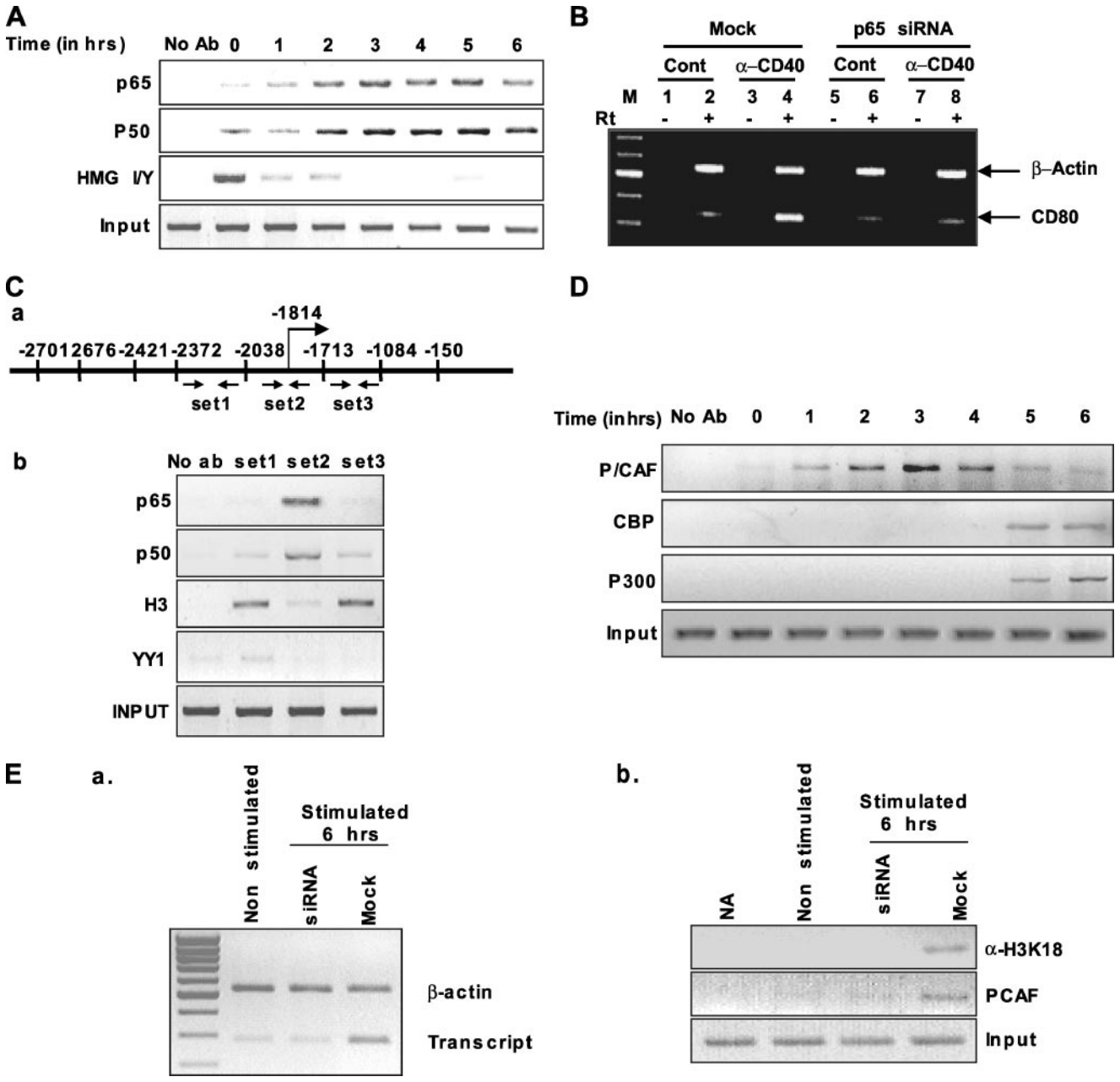

FIGURE 4. **Dynamic recruitment of activator and coactivator complexes in TS2-proximal region.** *A*, time-dependent ChIP analysis with the indicated antibodies and primers across the NF-κB-binding site in TS2-proximal region. The specificity of immunoprecipitation was ensured in parallel experiments where the primary antibody was omitted (*No ab*). *B*, RT-PCR with RNA isolated from the cells depleted of p65 using siRNA strategy (*lanes 1–4*, mock transfected; *lanes 5–8*, p65 siRNA-transfected). The efficiency of siRNA transfection was monitored by Western blotting (supplemental Fig. S1*D*). *C*, *panel a*, schematic representation of the Sau3AI sites on CD80 promoter and the primer pairs employed for the Scanning ChIP. *Panel b*, scanning ChIP assay, across the CD80 promoter, with the indicated antibodies and primer pairs following stimulation of the cells for 3 h with CD40. *D*, the kinetics of recruitment of P/CAF, P300, and CBP histone acetyltransferases as detected by the mononucleosome ChIP assays. Amplification results obtained with primers specific to nucleosome 1 are shown in the figure. *E*, *panel a*, RT-PCR analysis with the RNA isolated from unstimulated and either the mock or P/CAF siRNA-transfected cells stimulated with anti-CD40 antibody. P1/P2 primer pairs (illustrated in Fig. 1*A*) were employed for amplification. *Panel b*, ChIP analysis with antibody directed to the acetylated form of H3K18 in the unstimulated and, either mock or P/CAF siRNA-transfected cells, stimulated with anti-CD40 antibody for 6 h. *Cont*, control.

CD80 induction, we depleted cells of P/CAF by siRNA prior to their stimulation with anti-CD40. As shown in Fig. 4*E* (*panel a*), P/CAF suppression led to a complete inhibition of CD40-dependent CD80 induction, thus supporting a direct role for P/CAF in CD80 regulation. The acetylation of H3K18 was also blocked in P/CAF knock-down cells (Fig. 4*E*, *panel b*).

P-TEFb Recruitment Constitutes the Rate-limiting Step during CD80 Induction—Entry of Pol II into a productive elongation phase is also marked by the phosphorylation of serine residues in the CTD. Serine 2 and serine 5 residues of CTD are known substrates of P-TEFb and TFIIH, respectively, and the phosphorylation status of these residues is closely linked to the process of initiation and elongation (2, 3). Therefore, we next monitored the phosphorylation status of serine 2 and serine 5 of CTD and the resultant alterations as a function of cell stimulation. Phosphorylation of serine 5 could be detected even in unstimulated cells, although there was a further increase in this level by 5 h of stimulation (Fig. 5*A*). This is consistent with our

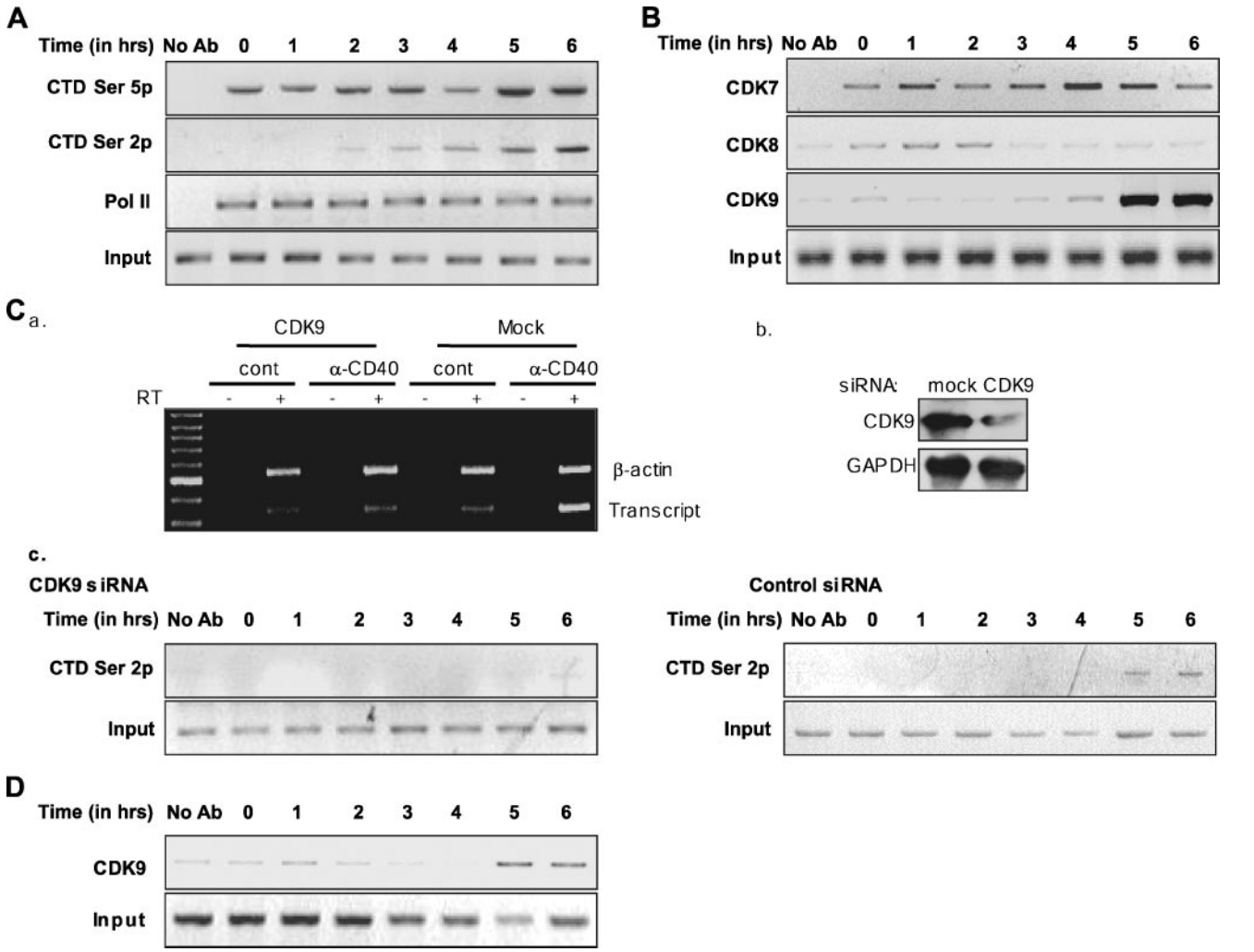

FIGURE 5. **Recruitment of CDK9 is critical for CD40-mediated induction of CD80 transcript from TS2.** *A*, ChIP analysis with the antibodies directed to Ser^2 and Ser^5 phosphorylated forms of CTD of Pol II, in a time-dependent manner. Primers across the TS2 start site were employed. *No Ab* represents the immunoprecipitation specificity controls. *B*, ChIP analysis to monitor the recruitment of CDK7, CDK8, and CDK9 in the cells stimulated for the indicated duration of time. *C*, *panel a*, RT-PCR with RNA isolated from the mock and CDK9 siRNA-transfected cells, stimulated for 6 h with anti-CD40 antibody. *Panel b*, Western blot analysis to monitor the steady state levels of CDK9 in the mock and CDK9 siRNA-transfected cells. *Panel c*, ChIP to monitor the status of serine 2 phosphorylation in either control or CDK 9 knock-down cells, stimulated with CD40 for the indicated duration of time. *D*, mononucleosome ChIP with CDK9 antibody to demonstrate the nucleosomal localization of CDK9. Primer pairs within the nucleosomal region were employed for amplification.

earlier finding in Fig. 3*C* that an initiation-competent form of Pol II was constitutively associated with the promoter-proximal region. In contrast, significant levels of serine 2 phosphorylation became detectable only between 4 and 5 h of stimulation with anti-CD40, correlating well with the time point at which CD80 mRNA begins to accumulate.

The time-dependent recruitment of the three CTD kinases was next examined. As shown in Fig. 5*B*, CDK7, a kinase subunit of TFIIH, was constitutively associated with the promoter with no significant change in its status upon stimulation. Similarly CDK8, a repressor that functions by phosphorylating CDK7, was also constitutively bound to the promoter, although stimulation led to its time-dependent dissociation (Fig. 5*B*). Interestingly, dissociation of CDK8 was succeeded by the recruitment of CDK9, the kinase subunit of P-TEFb. This was achieved between 4 and 5 h of stimulation, well in keeping with the observed kinetics of CTD serine 2 phosphorylation, as well as that of the accumulation of the CD80 transcript.

The above results suggested that CDK9 recruitment could likely constitute the critical step during CD40-mediated CD80 up-regulation. This could occur through the resulting phosphorylation of CTD at serine 2, thereby conferring elongation competence to Pol II. To test this, we employed siRNA to deplete cells of CDK9 prior to stimulation with anti-CD40. As shown in Fig. 5*C*, depletion of CDK9 (*panel b*) led to a complete inhibition of CD40-induced CD80 up-regulation (*panel a*). Further, there was also no increase in phosphorylation at serine 2 of CTD (*panel c*). Thus, CDK9 recruitment appears to represent the crucial and penultimate step during CD40-dependent up-regulation of CD80. A subsequent ChIP analysis on mononucleosome preparations revealed that CDK9 engagement involved its direct interaction with nucleosome 1 (Fig. 5*D*).

P-TEFb Recruitment Involves an Ordered Process—Our cumulative results revealed that CD40-mediated induction of CD80 expression involved the active recruitment of several dis-

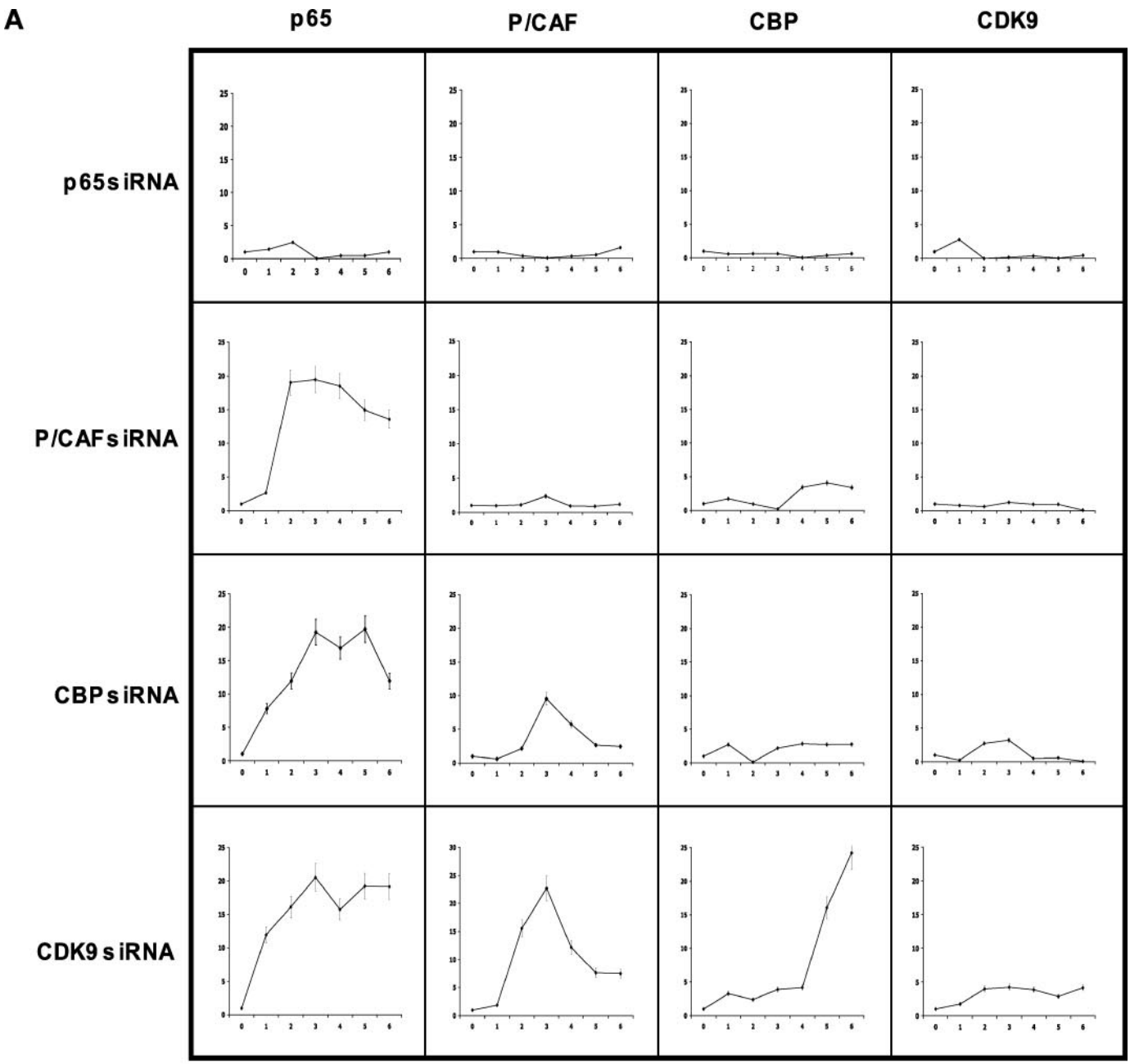

tinct proteins at the promoter. Whereas recruitment of both NF-κB and P/CAF occurred early after stimulation, that of CBP and P-TEFb took place close to the time point of appearance of the transcript. To explore for a possible relationship between these events, we selectively silenced these individual molecules by siRNA and then examined for the consequences.

Inhibition of expression of the p65 subunit of NF-κB resulted in a marked inhibition in the subsequent recruitment of P/CAF, CBP, and P-TEFb (Fig. 6*A*), thus revealing the critical role played by this transcription factor in the cascade of events that follow. Further, these findings also indicate that P/CAF recruitment occurs in an NF-κB-dependent manner. In comparison, specific suppression of P/CAF expression led to inhibition of the association of both CBP and P-TEFb, although that of NF-κB was unaffected (Fig. 6*A*). The silencing of CBP expression had no effect on the CD40-dependent association of NF-κB and P/CAF with the promoter, but activation-dependent engagement of P-TEFb was markedly inhibited (Fig. 6*A*). However, the inhibition of CDK9 expression did not affect the stimulus-dependent recruitment of p65, P/CAF, or CBP (Fig. 6*A*). These results, therefore, provide a resolution to the observed chronology of recruitment events and identify them to represent an ordered and interdependent process that likely leads to the cooperative assembly of a multimolecular complex. Thus, recruitment of NF-κB at the promoter facilitates P/CAF association. It is possible then that the resulting acetylation at nucleosome 1 provides the interacting site for the bromodomain of CBP, although NF-κB may also play a cooperative role in this process. It was, however, interesting that the subsequent recruitment of P-TEFb was dependent upon the histone acetyltransferases P/CAF and CBP, implicating that the acetylation status of nucleosome 1 was somehow relevant to this process. Our earlier findings that P-TEFb engagement involved its direct interaction with the nucleosome (Fig. 5*D*) provided additional support for such a possibility.

Recent studies have identified a double bromodomain-containing protein, Brd4, to be directly associated with a significant proportion of cellular P-TEFb (19). Such complexes were found to be devoid of inhibitory subunits such as HEX1M1, MAQ1, and 7SK RNA (20). It was therefore possible that the interaction of P-TEFb with the nucleosome, upon stimulation of cells with anti-CD40, was mediated through Brd4. To ascertain this we specifically silenced Brd4 expression by siRNA and stimulated the resulting cells with anti-CD40. Suppression of Brd4 expression also led to the specific inhibition of CD40-dependent recruitment of CDK9 at the CD80 promoter (Fig. 6*B*). A direct demonstration of the association of Brd4 with the nucleosome was, however, not possible because of the lack of commercially available antibodies against this protein. Nonetheless, these results do support the above-described process of ordered recruitment, which is initiated by the association of NF-κB and culminates with the recruitment of Brd4-complexed P-TEFb.

Finally, interaction of Pol II with the nucleosomal complex could be demonstrated by ChIP assays on mononucleosomal preparations, using antibodies against Pol II. As shown in Fig. 6*C* (*panel a*), nucleosome 1-bound DNA could also be immunoprecipitated and cross-linked to Pol II, but only after 5 h of stimulation of cells with anti-CD40. This timing is coincident with that for the induction of CD80 transcript, as well as that for CDK9 recruitment. Further, this interaction was abolished in cells that had first been depleted of CDK9 by siRNA (Fig. 6*C*, *panel b*), supporting the possibility that the interaction of Pol II with the nucleosome was likely mediated through involvement of CDK9.

DISCUSSION

Our present study contributes to the accumulating body of evidence reinforcing the relevance of transcription elongation as a regulatory event during Pol II transcription of a variety of both housekeeping and inducible genes. In addition, however, it also furnishes new insights into the level of intricacy that such regulation can entail. Pol II transcription elongation comprises the three stages of promoter escape, promoter-proximal pausing, and productive elongation, with either of the first two steps having the potential to be rate-limiting. As shown here, the basal transcriptional status of murine CD80 in the context of TS2 was characterized by aborted elongation because of arrest of Pol II in the promoter-proximal region. Release from its stalled position and consequent entry into the productive elongation phase, required stimulation of cells with anti-CD40. Surprisingly, however, we observed the presence of stimulus-dependent open complexes in the region ~200 bp downstream of the transcription start site, a likely indicator of the stalled polymerase in this region that resumed productive elongation post-stimulation. Promoter-proximal pausing usually results either from transcript slippage or from polymerase backtracking. Both of these phenomena are normally predominant within a RNA-DNA hybrid length of ~30 nt, by which point the TEC is stabilized (3). Although the likelihood of polymerase stalling at multiple sites on the promoter cannot be ruled out in view of the data presented here, CD80 appears to present a discrepant example where the polymerase stalling, at least in part, occurred subsequent to the formation of a stable TEC. In view of the known property of chromatin to impede elongation, a role for nucleosome 1 in inducing this paused state of the TEC may seem likely. Earlier studies have implicated a role for CDK7 in proximal promoter stalling of RNA Pol II (21). Our finding of the constitutive association of CDK7 with the TS2-proximal promoter may suggest a similar role for CDK7 in the present case.

FIGURE 6. **Ordered recruitment of the regulatory proteins following CD40 stimulation.** *A*, the results of tandem siRNA-ChIP experiments. ChIP analysis, with the indicated antibodies, was performed following transfection of the cells with p65, P/CAF, CBP, and CDK9 siRNA. The ethidium bromide-stained products of amplification, for each of the indicated sets, were quantitated and normalized for the values obtained for the respective inputs. Mean fold enrichment in the amplification products were plotted to obtain the results depicted in the figure. The efficiency of knock-down with each set of siRNA was monitored using Western blotting (not shown). *B*, ChIP assay performed in a time-dependent manner with the indicated antibodies following transfection of the cells with Brd4 siRNA. *C*, *panel a*, mononucleosome ChIP with the antibody directed to RNA polymerase II to demonstrate the time-dependent association of polymerase II with the nucleosome 1. *Panel b*, time-dependent mononucleosome ChIP assay performed with antibody directed to RNA polymerase II in the cells depleted of CDK9. *No Ab* represents the immunoprecipitation specificity control.

Consistent with the known requirements for the release of a paused TEC, TS2-initiated transcriptional activation of *CD80* also required the stimulus-dependent recruitment of P-TEFb at the promoter-proximal region. This then led to the hyperphosphorylation of CTD at serine 2 and the consequent resumption of transcription elongation. A surprising aspect of this process, however, was that this end point in fact represented the culmination of an intricately executed cascade of events. As suggested by the ChIP experiments, initiation of this cascade was marked by two distinct events. One of these was the anti-CD40 induced dissociation of HMGI(Y) from the promoter, whereas the other was the activation and recruitment of the p65-p50 heterodimer of NF-κB at its target site. Although CD40 ligation is known to activate NF-κB, our more recent results suggest that the induced dissociation of HMGI(Y) is mediated through its phosphorylation, in a protein kinase C-dependent manner.[4] It has been shown at previous instances, including our own results (18), that HMGI(Y) can function by modulating the promoter architecture. The fact that we could map at least one HMGI(Y)-binding site between the NF-κB-binding element and the nucleosome 1, which were separated by a few hundred nucleotides, raises an interesting possibility of a parallel regulatory pathway that could operate in the form of HMGI(Y)-driven promoter architecture. Clearly, as suggested by cumulative siRNA experiments, the NF-κB-dependent recruitment of P/CAF led to the activation of acetylation events at nucleosome 1. It is likely that such a structural framework provided by the promoter architecture also accounts for the regio-selectivity of NF-κB-associated P/CAF where acetylation at nucleosome 1, but not at either nucleosome 2 or nucleosome 3, was specifically initiated.

In view of the fact that TEC pausing occurred close to nucleosome 1, we anticipated remodeling at the latter to serve as the regulatory step. However, repeated experiments failed to yield any evidence for nucleosome remodeling, when monitored at the level of either restriction enzyme accessibility or nucleosome sliding (data not shown). On the contrary, our results suggest that nucleosome 1 primarily functioned by serving as a locus for the regulated recruitment of P-TEFb. Thus, as revealed from the combination of our sequential siRNA and mononucleosome ChIP experiments, the P/CAF-dependent acetylation of nucleosome 1 paved the way for the subsequent engagement of CBP. This led to an increase in the spectrum of H3 lysine residues acetylated, and the hyperacetylated nucleosome then provided the docking site for a Brd4-complexed form of P-TEFb. Finally, tethering of P-TEFb to nucleosome 1 facilitated its interaction with CTD and the consequent initiation of hyperphosphorylation of the latter at serine 2.

The events outlined above, consisting of a cooperative process of ordered cofactor recruitments, are reminiscent of the mechanisms delineated for the preinitiation step of transcription. However, whereas such an elaborate process is required to ensure target-specific assembly of the preinitiation complex in such cases, the end result here was to facilitate the release of a stalled TEC. In view of the increasing number of genes that are now being found to be controlled at the level of transcription elongation (22), it is not unreasonable to expect the existence of mechanisms that also regulate the expression of such genes in a specific manner. Thus, by revealing the level of intricacy that can be involved during the release of a stalled TEC, our present report provides an insight into how such specificity may be achieved.

[4] M. Sharma, A. A. George, B. N. Singh, N. C. Sahoo, and K. V. S. Rao, unpublished results.

REFERENCES

1. Shilatifard, A. (1998) *FASEB J.* **12,** 1437–1446
2. Sims, R. J., III, Belotserkovskaya, R., and Reinberg, D. (2004) *Genes Dev.* **18,** 2437–2468
3. Saunders, A., Core, L. J., and Lis, J. T. (2006) *Nat. Rev. Mol. Cell. Biol.* **7,** 557–567
4. Dahmus, M. E. (1996) *J. Biol. Chem.* **271,** 19009–19012
5. Palancade, B., and Bensaude, O. (2003) *Eur. J. Biochem.* **270,** 3859–3870
6. Prelich, G. (2002) *Eukaryot. Cell* **1,** 153–162
7. O'Brien, T., Hardin, S., Greenleaf, A., and Lis, J. T. (1994) *Nature* **370,** 75–77
8. Komarnitsky, P., Cho, E. J., and Buratowski, S. (2000) *Genes Dev.* **14,** 2452–2460
9. Cheng, C., and Sharp, P. A. (2003) *Mol. Cell. Biol.* **23,** 1961–1967
10. Sharpe, A. H., and Freeman, G. J. (2002) *Nat. Rev. Immunol.* **2,** 116–126
11. Selvakumar, A., White, P. C., and Dupont, B. (1993) *Immunogenetics* **38,** 292–295
12. Borriello, F., Freeman, G. J., Edelhoff, S., Disteche, C. M., Nadler, L. M., and Sharpe, A. H. (1994) *J. Immunol.* **153,** 5038–5048
13. Weinmann, A. S., Plevy, S. E., and Smale, S. T. (1999) *Immunity* **11,** 665–675
14. Soutoglou, E., and Talianidis, I. (2002) *Science* **295,** 1901–1904
15. Narlikar, G. J., Fan, H. Y., and Kingston, R. E. (2002) *Cell* **108,** 475–487
16. Krumm, A., Meulia, T., Brunvand, M., and Groudine, M. (1992) *Genes Dev.* **6,** 2201–2213
17. Donepudi, M., Raychaudhuri, P., Bluestone, J. A., and Mokyr, M. B. (2001) *J. Immunol.* **166,** 6491–6499
18. George, A. A., Sharma, M., Singh, B. N., Sahoo, N. C., and Rao, K. V. (2006) *EMBO J.* **25,** 811–821
19. Jang, M. K., Mochizuki, K., Zhou, M., Jeong, H. S., Brady, J. N., and Ozato, K. (2005) *Mol. Cell* **19,** 523–534
20. Marshall, R. M., and Grana, X. (2006) *Front. Biosci.* **11,** 2598–2613
21. Schwartz, B. E., Larochelle, S., Suter, B., and Lis, J. T. (2003) *Mol. Cell. Biol.* **23,** 6876–6886
22. Kim, T. H., Barrera, L. O., Zheng, M., Qu, C., Singer, M. A., Richmond, T. A., Wu, Y., Green, R. D., and Ren, B. (2005) *Nature* **436,** 876–880